LA-UR -93-2449

Conf-930718--2

Los Alamos National Laboratory is operated by the University of California for the United States Department of Energy under contract W-7405-ENG-36

TITLE: **EXPERIMENTAL STUDY OF A SHOCK ACCELERATED THIN GAS LAYER**

AUTHOR(S): **J.W. JACOBS, D.G. JENKINS, D.L. KLEIN, R.F. BENJAMIN**

SUBMITTED TO: **NINETEENTH INTERNATIONAL SYMPOSIUM ON SHOCK WAVES, JULY 26-30, 1993 AT UNIVERSITE DE PROVENCE, MARSEILLE, FRANCE**

MASTER

Los Alamos National Laboratory
Los Alamos, New Mexico 87545

Experimental Study of a Shock Accelerated Thin Gas Layer

J. W. Jacobs
Aerospace and Mechanical Engineering, University of Arizona, Tucson AZ 85721

D. G.Jenkins, D. L. Klein, R. F. Benjamin
Los Alamos National Laboratory, Los Alamos, NM 87545

Abstract. Planar laser-induced fluorescence imaging is utilized in shock-tube experiments to visualize the development of a shock-accelerated thin gas layer. The Richtmyer-Meshkov instability of both sides of the heavy gas layer causes perturbations initially imposed on the two interfaces to develop into one of three distinct flow patterns. Two of the patterns exhibit vortex pairs which travel either upstream or downstream in the shock tube, while the third is a sinuous pattern that shows no vortex development until late in its evolution. The development of the observed patterns as well as the growth in the layer thickness is modeled by considering the dynamics of vorticity deposited in the layer by the shock interaction process. This model yields an expression for the layer growth which is in good agreement with measurements.

1. Description of phenomena

The interaction of a shock wave with a perturbed interface separating fluids of different densities produces growth of the perturbations. This interfacial fluid instability, known as the "Richtmyer-Meshkov" (R-M) instability, is the shock-accelerated analog of the Rayleigh-Taylor (R-T) instability, and produces similar flow patterns. However, when two nearby interfaces undergo R-M instability, the flow patterns are more complex than expected from single-interface results. We observe experimentally that the shock interaction with the two nearby interfaces of a thin gas layer produces multiple flow evolutions, as first reported by Jacobs et al. (1993). The shocked layer evolves into one of three distinct patterns, indicating a flow bifurcation. The multiple patterns may be related to subtle differences in initial conditions, but we are unable to detect these differences.

The role of vorticity in shock accelerated flows is recognized as important (Picone and Boris 1988). Vorticity generated in R-T and R-M instabilities by the misalignment of pressure and density gradients is manifest as vortical structures during intermediate and late time development. For R-M growth the dominant pressure gradient is in the shock wave, and the dominant density gradients occur at the interfaces. Motivated by our experimental observations, we have developed a simple vortex model that assumes vorticity produced by the shock

interaction becomes a row of line vortices. The expression for the growth of the perturbed layer derived from our model gives predictions in good agreement with our measurements.

2. Experimental technique

We image a cross section of the thin gas layer with PLIF (planar laser-induced fluorescence) to enable visualization of the two nearby interfaces undergoing R-M instability. This technique enables the observation of the flow without the distortion caused by boundary effects seen during our (as well as others) attempts to use Schlieren imaging to detect this flow. The heavy gas layer (i.e., the "gas curtain") is created within the shock tube by a spatially modulated planar SF_6 jet which flows vertically downward from a contoured nozzle. A bottom exhaust removes excess SF_6. The cross section of the layer has a varicose profile, designed to impose ripples on both upstream and downstream surfaces. After a horizontally-moving Mach-1.2 shock wave accelerates the layer, a pulsed laser sheet illuminates the interfacial region at a preset delay. The cross section is made visible by mixing a small amount of a fluorescent tracer (diacetyl) into the SF_6 stream. We capture one fluorescent image per experiment on an intensified CCD camera and store it in a desktop computer. Images from different experiments are sorted into the three patterns which form "ensemble cinemas" of the event. Both PLIF and gas curtain methods were adapted from Jacobs' (1992) experiments studying shock-accelerated cylindrical jets. The use of diacetyl is justified by recent results of Budzinski (1992). Further experimental details are described in Jacobs et al. (1993) and subsequent journal publications.

3. Observations

We observe three flow patterns evolving from the shock-accelerated, initially varicose layer, shown by the ensembles of fluorescent images in figure 1. Two of the patterns show the presence of vortex pairing during the first millisecond after shock acceleration. The pairing is manifest as mushroom-shaped profiles. The pattern with mushrooms on the upstream side occurs during about 50% of the events, while the pattern with "downstream mushrooms" occurs only 10% of the time. The third pattern is a sinuous pattern, and occurs about 40% of the time. We are unable to predict or control which pattern will emerge on any given event.

Figure 2 is a plot of the width of the layer vs. time for these experiments. The width is the measured distance between the extremes of the SF_6/diacetyl signal along the shock wave direction. Despite considerable scatter in this data, upstream mushrooms show substantially faster growth than do the other two patterns

4. Interpretation and Analysis

The prominence of vortical patterns in figure 1 motivates our vortex model which uses a row of vortices to describe intermediate- and late-time instability growth. Because the strength of these vortices is determined during the shock interaction, we must first examine the initial stage of the instability. This stage is well characterized by linear Richtmyer-Meshkov instability theory. Consider a planar fluid layer with thickness 2h and density ρ_2 surrounded by fluid of density ρ_1. If periodic perturbation amplitudes on each of the two interfaces have the form,

$$\eta_1 = a_1(t) \cos kx \tag{1}$$

$$\eta_2 = a_2(t) \cos kx \tag{2}$$

then the growth of these perturbations is given by (Mikaelian 1985).

$$\frac{da_1}{dt} + \frac{da_2}{dt} = k A_t \Delta V (a_{1,0} - a_{2,0}) \tag{3}$$

$$\frac{da_1}{dt} - \frac{da_2}{dt} = k A_c \Delta V (a_{1,0} + a_{2,0}). \tag{4}$$

where

$$A_t = \frac{\rho_2 - \rho_1}{\rho_1 + \rho_2 \tanh kh} \tag{5}$$

$$A_c = \frac{\rho_2 - \rho_1}{\rho_1 + \rho_2 \coth kh} \tag{6}$$

and ΔV is the velocity change induced by the impulsive acceleration. For a varicose type of initial perturbation, the initial amplitudes $a_{1,0}$ and $a_{2,0}$ are related by, $a_{2,0} = -a_{1,0} \equiv -a_0$, thus

$$\frac{da_1}{dt} = \frac{da_2}{dt} = k A_t \Delta V a_0. \tag{7}$$

Similarly for a sinuous type perturbation, $a_{2,0} = a_{1,0} = a_0$, and

$$\frac{da_1}{dt} = -\frac{da_2}{dt} = k A_c \Delta V a_0. \tag{8}$$

Therefore, as expected from linear R M theory for a single interface, the disturbance on the light heavy interface (i.e. the upstream interface in the experiments) grows linearly with time, and the disturbance on the light heavy interface (i.e. the downstream interface in the experiments) inverts phase and then grows. Consequently, an initially varicose shaped layer should evolve into a sinuous shape and an initially sinuous shaped layer should evolve into a varicose shape.

Equations (7) and (8) differ from the equivalent expressions obtained for a single interface in that the modified Atwood numbers A_t and A_c depend on the layer thickness. However, if $kh >> 1$ (i.e., layer thickness $\leq$ perturbation wavelength) then A_t and A_c are equal to the standard definition of the Atwood number. Thus for sufficiently large values of kh the two interfaces act independently. It is interesting to note that as the layer thickness approaches zero, $A_t \rightarrow (\rho_2 - \rho_1)/\rho_1$ and $A_c \rightarrow 0$. Thus, growth is enhanced for a varicose disturbance on a heavy layer and inhibited for a varicose light layer. But growth of a sinuous layer is always inhibited and is zero in the limit of an infinitely thin layer.

The vorticity generated by shock interaction will lie on the boundaries of the layer, and will vary periodically along its length. Assuming the boundary separating the two fluids is sharp, the vorticity is concentrated in a thin sheet on the boundary. The strength of each of these sheets (γ_1 and γ_2) is equal to the jump in tangential velocity across each of the two boundaries, as calculated from linear theory:

$$\gamma_1 = \gamma_2 = -(1 + \tanh kh)\, A_t\, k\, a_0\, \Delta V \sin kx \tag{9}$$

for an initially varicose layer, and,

$$\gamma_1 = -\gamma_2 = -(1 + \coth kh)\, A_c\, k\, a_0\, \Delta V \sin kx. \tag{10}$$

for a sinuous layer.

The jet technique used in our experiments results in a diffuse interface which causes the vorticity to be distributed throughout the layer. Thus, the result of the shock interaction is not to produce two sheets of vorticity, but a distribution more like a row of diffuse vortices with alternating sign, and spacing π/k. If it is assumed that the vorticity contained in the vortex sheets is concentrated in a row of line vortices with strength $\pm K$, then for the present experiments which have a varicose initial shape,

$$K = -\frac{2}{\pi}(1 + \tanh kh)\, A_t\, \Delta V\, a_0. \tag{11}$$

The row of vortices will induce motion given by the stream function,

$$\psi = \frac{1}{2} K \ln \left| \frac{\cosh(ky) + \sin(kx)}{\cosh(ky) - \sin(kx)} \right| \tag{12}$$

which will distort the layer. Near the vortex cores the induced velocity will act to wrap the layer around the vortices, but in the regions between the vortices the induced motion works to push the layer in a direction perpendicular to the row. After a period of time, the spreading of the layer

will be predominantly caused by the fluid motion near $x = 0, \pm\pi/k, \pm 2\pi/k, \ldots$. Evaluating the velocity at these points and then integrating to obtain the layer width yields,

$$w = 2 \sinh^{-1}\left[\frac{2}{\pi} (1 + \tanh(kw_o/2))\, k^2 A_t \Delta V a_0 t + \sinh(kw_o/2) \right] \qquad (13)$$

where w_0 is a measure of the average initial layer width. Note that for sufficiently large values of x, $\sinh^{-1}(x) \equiv \ln(2x)$; therefore, the late time growth of the layer is logarithmic in time. Equation (13) was evaluated using known or measured values of k, A_c, ΔV and estimates of w_0 and a_0 and is shown in Fig. 2 along measurements of the layer width and the result for the linear stability analysis (equation 7). The theory is in quite good agreement with the data and is substantially better model than linear theory.

A row of equidistant vortices is well known to be unstable (von Karman, in Lamb 1945 pp 225-229). One mode of instability can be generated by uniformly displacing every other vortex along the row, producing a row of vortex pairs. Vortices induce motion inversely proportional to their separation. Displacing every other vortex closer to its neighbor will cause the entire row of vortices to move in a direction perpendicular to the layer. Thus, small lateral perturbations to the initial distribution of vortices in our experiments can generate vortex pairs (or mushrooms) which travel upstream or downstream. The type of mushroom (upstream or downstream) would then be determined by whether the vortex pairing occurs at the thick or thin parts of the layer. If the vortex pairing occurs within the thick regions, upstream mushrooms will form as shown in Fig. 1a. Vortex pairing occurring within the thin regions will produce downstream mushrooms (Fig. 1b). Because the initial distribution of vorticity is not discrete, but is in reality distributed regions of vorticity, a nearly uniform vortex spacing will cause the distributed vortex cores to be strained by the induced flow field. This stretching will act to pull apart the vortex cores, thus inhibiting roll-up and producing what we observe as the sinuous mode (Fig. 1c).

5. Conclusions

The interaction of a shock wave with the two nearby interfaces of a thin gas layer produces flow patterns unexpected from single-interface, Richtmyer-Meshkov instability studies. Using PLIF imaging, we observe three distinct flow patterns which we cannot control or predict on a given experiment. Our simple model, which approximates the shock generated vorticity as a row of line vortices and uses results from perturbation theory to estimate vortex strengths, predicts instability growth consistent with our experimental observations. The measured growth is far less than predicted by linear perturbation theory.

6. Acknowledgements

This research has been supported by the US Department of Energy, Contract No. W-7405-ENG-36. We are grateful to R. Reinovsky and J. Shaner for encouragement.

References

Budzinski JM (1992) PhD thesis, California Institute of Technology, Pasadena, CA

Jacobs JW, Jenkins DG, Klein DL, Benjamin RF (1993) Instability growth patterns of a shock-accelerated thin fluid layer. Phys. Rev. Lett. 70:583

Jacobs JW (1992) Shock induced mixing of a light gas cylinder. J. Fluid Mech. 234:629

Lamb H (1945) Hydrodynamics. Dover, New York

Mikaelian K (1985) Richtmyer-Meshkov instabilities in stratified fluids. Physical Review A 31:410

Picone JM, Boris JP (1988) Vorticity generation by shock propagation through bubbles in a gas. J Fluid Mech. 189:23

Figure Captions

1. Three ensembles of PLIF images representing time sequences in the development of the: (a) upstream mushroom, (b) downstream mushroom, and (c) sinuous flow patterns. Interframe time is approximately 100 μs. Brighter or darker regions indicate stronger fluorescent emission and therefore higher concentrations of SF_6 and diacetyl. Each image is taken on a different experiment.

2. Measured growth of the SF_6-layer width is well estimated by our vortex model, but poorly described by linear theory. Each datapoint corresponds to a different experiment, and the shot-to-shot variability is the dominant source of scatter among the datapoints.

Figure 1

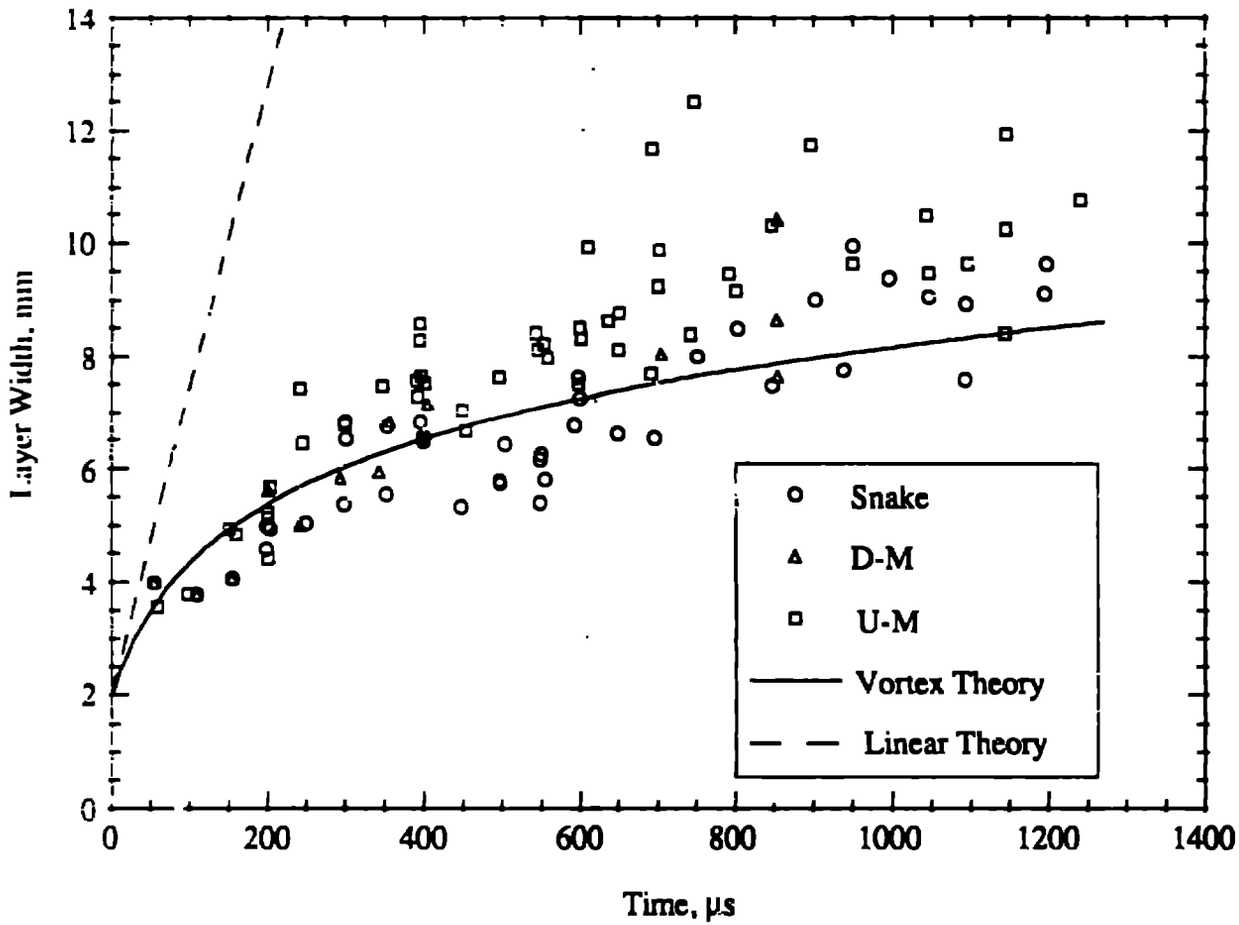
Layer Width, mm
Time, μs
0
2
4
6
8
10
12
14
0
200
400
600
800
1000
1200
1400
Snake
D-M
U-M
Vortex Theory
Linear Theory

Figure 2